Cite this as: Polyhedron 185 (2020) 114565
https://doi.org/10.1016/j.poly.2020.114565

# Sonochemical synthesis of two nanoscale Co(II) coordination compounds: Facile fabrication of $Co_3O_4$ nanoparticles with various morphologies

Arash Farahmand Kateshali [a], Janet Soleimannejad [a,⇑], E. Carolina Sañudo [b]

[a] School of Chemistry, College of Science, University of Tehran, P.O. Box 14155-6455, Tehran, Iran
[b] Departament de Química Inorgànica i Orgànica, Secció de Química Inorgànica, Universitat de Barcelona, Av. Diagonal 645, 08028 Barcelona, Spain

a r t i c l e i n f o

*Article history:*
Received 1 March 2020
Accepted 15 April 2020
Available online 18 April 2020

*Keywords:*
Cobalt (II)
Cobalt oxide
Nanoparticles
2,3-Pyrazinedicarboxylic
Magnetic property

a b s t r a c t

Two new nanoscale cobalt(II) coordination compounds, $(adH)_3[Co(Hpzdc)(pzdc)_2].6H_2O$ (1) and $[Co(pzdc)_2(H_2O)_2]_n$ (2) (where $H_2$pzdc is 2,3-pyrazinedicarboxylic acid and ad is adenine), were synthesized using a sonochemical process and characterized *via* scanning electron microscopy (SEM), X-ray powder diffraction (XRPD) and FT-IR spectroscopy. The structural characterization of 1 through single crystal X-ray diffraction revealed that it consists of a 0D coordination compound in which Co(II) ion is six-coordinated by two $pzdc^{2-}$ and one $pzdcH^-$ ligands. Compound 2 however, is a 1D coordination polymer (CP) and was found to be a perfect precursor for $Co_3O_4$ nanoparticles. Changes in the morphology and size of the nanoparticles have been induced by altering the calcination temperature in the range of 400 to 850 °C. Furthermore, the magnetic behavior of 2 was studied and compared with its single crystal counterpart.

## 1. Introduction

The design and synthesis of cobalt-based coordination compounds has attracted researchers' attention due to the diversity of their structural types, architectures, topologies, as well as important properties resulting in great potential applications such as biomarker, catalyst, super-capacitor, chemosensor and single molecular magnets [1–6]. By scaling down the size of coordination compounds to the nanoscale, these compounds will further benefit from certain attributes associated with nanomaterials *e.g.* high surface to volume ratio, leading to the introduction of a unique set of advantages that can expand the breadth of their applications [7,8].

Among the available methods to synthesize nanoscale coordination compounds, sonochemical synthesis provides an efficient, low-cost, facile and versatile synthesis tool. It is purely based upon the effects of the mechanical energy transferred through the medium, including the formation, growth, and implosive collapse of bubbles (acoustic cavitation) in a liquid. Upon the collapsing of bubbles, huge amounts of heat are released and extraordinary conditions (extremely high temperatures and pressures) are established for less than a nanosecond which in turn allows for the synthesis of a wide variety of nano-sized materials [9,10].

Following our prior work on the synthesis, structural analysis and applications of nanocrystalline CPs [11–13], here we report two new nanosized cobalt-based coordination compound $(adH)_3[Co(Hpzdc)(pzdc)_2].6H_2O$ (1) and $[Co(pzdc)_2(H_2O)_2]_n$ (2). The approach we have used is based on the proton transfer (PT) process between a carboxylic acid with an amine, which leads to the production of a self-associating ion pair system that reacts with metal ion and results in a coordination compound. Compound 1 and 2 are two different products resulting from the same metal ion and PT system but differing initial molar ratios. The acid used in the preparation of these compounds is 2,3-pyrazinedicarboxylic acid which has been employed widely due to its multiple coordination modes and the steric hindrance between the carboxylate groups which helps to increase the dimensionality of the assembled covalent networks with interesting properties [14,15].

Adenine as a member of nucleobases family is attractive. It is capable of coordination through multiple positions, establishes p-p stacking owing to its planarity and p-conjugated structure, and presents many edges capable of establishing complementaryH-bonding interactions that provide reliable synthons. These non- covalent interactions stabilize network solids that are useful advanced materials [16]. The biocompatibility of these ligands also provides a stimulus for assessing novel biological applications. Pro- tonated nucleobases play a crucial role in nucleic acid chemistry,

⇑ Corresponding author.
*E-mail address:* janet_soleimannejad@khayam.ut.ac.ir (J. Soleimannejad).

for instance in acid-base catalysis, and they are present in many biochemical processes *e.g.* enzymatic reactions [17].

Compound **2** was also found to be a low-cost precursor for $Co_3O_4$ nanoparticles and interesting morphologies were obtained upon altering the conversion temperature. Among the useful nanoscale metal oxides, nanoscale $Co_3O_4$ is an important antiferromagnetic *p*-type semi-conductor with a spinel crystal structure taken from a cubic close packing array of oxide ions. It is widely used in various fields of application such as catalysis, medicine, electrochromic devices, gas sensors, magnetism, and lithium-ion batteries [18,19].

We also studied the magnetic properties of **2** and compared the result with its single crystal analogue (**2'**).

## 2. Experimental

### 2.1. Materials and physical techniques

All chemicals for the synthesis of the compound were obtained in grade commercial samples. Ultrasonic syntheses and reactions were carried out on a SONIC 3MX, (maximum 160 W at 37 kHz). Elemental analysis (C, H and N) was performed using Vario-EL-III elemental analyzer. FTIR spectra were recorded with a Nicolet Protégé 460 spectrometer using the KBr disk technique. Scanning Electron Microscopy (SEM) was performed on a KYKY EM-3200. The simulated XRD powder pattern based on single crystal data was prepared using the Mercury software. PXRD patterns were collected in a PANalytical X'Pert Pro diffractometer via glinting copper radiation (Cu Kα = 1.5418 Å) with an X'Celerator detector that was operated at 40 mA and 45 kV. Obtained profiles were received in the 5° < 2θ < 50° range with a step size of 0.012. Magnetic measurements were done on crushed polycrystalline, vacuum dried samples using a SQUID magnetometer equipped with a 5 T magnet, and diamagnetic corrections were applied using Pascal's constants (Done at the Servei de Mesures Magnètiques of CCiT-UB). Single crystal X-ray data was collected at 298 K for the compounds on a Bruker CCD diffractometer using monochromatized MoKα radiation (λ = 0.71073 Å). The data was corrected for absorption using empirical methods (SADABS) based upon symmetry-equivalent reflections combined with measurements at different azimuthal angles [20,21]. To solve the structures, direct methods using SHELXS-97 were applied that determined the positions of almost all non-hydrogen atoms [22]. The materials were purified using SHELXL with the anisotropic thermal displacement parameters. The hydrogen atoms of the aromatic ring were refined with the riding model. The data of compound **1'** were deposited in the Cambridge crystallographic data center with deposition number CCDC 1843011. The detailed crystallographic data and structure refinement parameters are summarized in Table 1.

### 2.2. Synthesis of $(adH)_3[Co(Hpzdc)(pzdc)_2].6H_2O$ (1)

To prepare **1**, an aqueous solution of $pzdcH_2$ (25 ml, 0.04 M) and adenine (25 ml, 0.04 M) was placed in an ultrasonic bath and irradiated with a power of 160 W at 60 °C. Into this aqueous solution, a solution of cobalt (II) acetate (25 ml, 0.02 M) was added in a dropwise manner. The obtained precipitates were filtered off, washed with water and then dried in air (yield 53%), m.p. 210 °C. Anal. calc. for $C_{33}H_{35}CoN_{21}O_{18}$: C, 36.76; H, 3.29; N, 27.35. Found: C, 36.72; H, 3.29; N, 27.33%. IR ($cm^{-1}$) selected bands: 679 (s), 756 (s), 940 (s), 1083 (s), 1324 (s), 1486 (s), 1612(s), 3017 (br) and 3500 (br).

Table 1
Crystal data and refinement details for compound **1'**.

| Empirical formula | $C_{33}H_{35}CoN_{21}O_{18}$ |
|---|---|
| Formula weight | 1072.71 |
| Temperature | 298(2) K |
| Wavelength | 0.71073 Å |
| Crystal system | Triclinic |
| Space group | $P\bar{1}$ |
| Unit cell dimensions | $a$ = 8.2031(16) Å |
| | $b$ = 16.165(3) Å |
| | $c$ = 17.153(3) Å |
| | α = 99.12(3)° |
| | β = 94.66(3)° |
| | γ = 102.75(3)° |
| Volume | 2174.4(7) Å$^3$ |
| Z | 2 |
| Density (calculated) | 1.638 Mg m$^{-3}$ |
| Absorption coefficient | 0.497 mm$^{-1}$ |
| F(0 0 0) | 1102 |
| Theta range for data collection | 1.21 to 27.88° |
| Index ranges | $-10 \le h \le 10$ |
| | $-21 \le k \le 21$ |
| | $-22 \le l \le 22$ |
| Reflections collected | 22,192 |
| Independent reflections | 9635 [$R$(int) = 0.0618] |
| Absorption correction | Semi-empirical from equivalents |
| Max. and min. transmission | 0.9247 and 0.8899 |
| Refinement method | Full-matrix least-squares on F$^2$ |
| Data / restraints / parameters | 9635 / 0 / 663 |
| Goodness-of-fit on F$^2$ | 1.079 |
| Final $R$ indices [I > 2sigma(I)] | $R1$ = 0.0743, w$R2$ = 0.1605 |
| $R$ indices (all data) | $R1$ = 0.1104, w$R2$ = 0.1830 |

### 2.3. Synthesis of $(adH)_3[Co(Hpzdc)(pzdc)_2].6H_2O$ single crystals (1')

A solution of $pzdcH_2$ (0.033 g, 0.2 mmol) and adenine (0.027 g, 0.2 mmol) in water (5 ml) was refluxed for one hour. A solution of $Co(NO_3)_2 \cdot 6H_2O$ (0.03 g, 0.1 mmol) in 2 ml water was added to this solution and refluxed for an additional 2 h. The resulting solution was then filtered and left to sit at room temperature. Single crystals suitable for X-ray crystallography were obtained by slow evaporation of the solvent, after one week (yield 62%), m.p. 212 °C. Anal. calc. for $C_{33}H_{35}CoN_{21}O_{18}$: C, 36.81; H, 3.30; N, 27.40. Found: C, 36.75; H, 3.30; N, 27.35%. IR ($cm^{-1}$): 644 (s), 939 (s), 1063 (s), 1116 (s), 1341 (s), 1424 (s), 1564 (s), 1612 (s), 3327 (br) and 3500 (br).

### 2.4. Synthesis of $\{[Co(pzdc)_2(H_2O)_2].H_2O\}_n$ (2)

Compound **2** was initially synthesized in the presence of adenine but after obtaining its single crystals (**2'**, section 2.6) in the absence of adenine, the following method was developed.

To prepare **2**, an aqueous solution of $pzdcH_2$ ligand (20 ml, 0.015 M) was placed in an ultrasonic bath and irradiated with a power of 160 W at 55 °C. Into this aqueous solution, a solution of cobalt(II) acetate (20 ml, 0.015 M) was added in a dropwise manner. The obtained precipitates were filtered off, washed with water and then dried in air (yield 57%), m.p. > 303 °C. Anal. calc. for $C_6H_{10}CoN_2O_8$: C, 24.22; H, 3.37; N, 9.40. Found: C, 24.16; H, 3.37; N, 9.28%. IR ($cm^{-1}$): 752 (s), 789 (s), 1044 (s), 1170 (s), 1218 (m), 1377 (s), 1435 (s), 1632 (s) and 3386 (br).

### 2.5. Synthesis of $\{[Co(pzdc)_2(H_2O)_2].H_2O\}_n$ single crystals (2') (a)

A solution of $pzdcH_2$ (0.016 g, 0.1 mmol) and adenine (0.013 g, 0.1 mmol) in 5 ml of water was refluxed for one hour. A solution of $Co(NO_3)_2 \cdot 6H_2O$ (0.03 g, 0.1 mmol) in 2 ml of water was added to this solution and refluxed for an additional 2 h. The prepared solution was filtered and left to sit at room temperature. Upon slow

evaporation of the solvent, single crystals suitable for X-ray crystallography were obtained after 3 days (yield 51%), m.p. > 300 °C. Anal. calc. for $C_6H_{10}CoN_2O_8$: C, 24.26; H, 3.39; N, 9.43. Found: C, 24.21; H, 3.39; N, 9.31%. IR ($cm^{-1}$): 686 (s), 745 (s), 886 (s), 1045 (s), 1120 (s), 1377 (s), 1430 (s), 1595 (s), 1632 (s) and 3375 (br).

### 2.6. Synthesis of $\{[Co(pzdc)_2(H_2O)_2].H_2O\}_n$ single crystals ($2^{\emptyset}$) (b)

The method used here is exactly the same as procedure a (section 2.5.) except that in this case adenine has not been used. (yield 55%), m.p. > 300 °C. Anal. calc. for $C_6H_{10}CoN_2O_8$: C, 24.26; H, 3.39; N, 9.43. Found: C, 24.21; H, 3.39; N, 9.31%. IR ($cm^{-1}$): 686 (s), 745 (s), 886 (s), 1045 (s), 1121 (s), 1377 (s), 1429 (s), 1592 (s), 1632 (s) and 3375 (br).

### 2.7. Preparation of cobalt oxide ($Co_3O_4$) nanoparticles

Nanoparticles of cobalt oxide were produced *via* thermal conversion of 2 at different temperatures of 400, 600, 800, and 850 °C in a static atmosphere of air for 5 h (yield 76, 75, 72, 68% for 400, 600, 800, 850 °C, respectively).

## 3. Results and discussion

Nanoscale aggregates of 1 and 2 were synthesized utilizing the ultrasonic technique (Scheme 1s) and their size and morphology were examined by scanning electron microscopy (SEM), which revealed mainly nano-sized, ball like morphologies (Fig. 1 and 1s). However, a full characterization of 1 and 2 required synthesis of their single crystals ($1^{\emptyset}$ and $2^{\emptyset}$, respectively) which is discussed in the following section.

### 3.1. Crystal structures of compound $1^{\emptyset}$ and $2^{\emptyset}$

Orange block-shaped single crystals of compound $1^{\emptyset}$ were prepared using an ad:$H_2$pydz:Co stoichiometry of 2:2:1. X-ray crystallography revealed that the reaction of adenine and 2,3-pyrazinedicarboxylic acid with cobalt(II) nitrate hexahydrate leads to the formation of a new 0D coordination compound of $(adH)_3[Co(Hpzdc)(pzdc)_2].6H_2O$ ($1^{\emptyset}$). The asymmetric unit of $1^{\emptyset}$ contains one Co(II) ion coordinated by two $pzdc^{2-}$ and one $pzdcH^-$ ligands, three protonated adenine species $(adH)^+$ and six uncoordinated water molecules. The cobalt(II) ion which is *hexa*-coordinated by three nitrogen atoms (N1, N3, and N5) and three oxygen atoms (O1, O5, and O9) from two $pzdc^{2-}$ and one $pzdcH^-$ ligands, exhibits a distorted octahedral geometry (Table 1s). The coordination environment of Co(II) ion with the atom numbering scheme is illustrated in Fig. 2.

It is noteworthy that, in compound $1^{\emptyset}$, adenine molecules are present in the form of protonated 1H,9H-adeninium cations. Adenine offers five available proton attachment sites with the basicity order of N9 > N1 > N7 > N3 > N10 (Scheme 2s) and the protonated 1H,9H-adeninium form is in agreement with the relative basicity of the *N*-rich nucleobase. These cations are responsible for charge balance of the 3D network.

There are relatively strong hydrogen bonds in compound $1^{\emptyset}$ with the D-- -A interaction distance ranging from 2.653(5) Å to 3.444(10) Å (Table 2s). Stacking interactions such as the p--p interactions between pzdc rings with a distance of 3.480 Å, (Fig. 2s), the NH-- -p interactions between adenine rings with distances of 3.387, 3.839 and 3.628 Å and the p--p interactions between adenine rings with a distance of 3.864 Å (Fig. 3s) have an important role in the self-assembly and molecular recognition process. The packing diagram of compound $1^{\emptyset}$ is shown in Fig. 4s.

Orange block-shaped crystals of compound $2^{\emptyset}$ were initially prepared using an ad:$H_2$pydz:Co stoichiometry of 1:1:1 over a period of three days. X-ray crystallography revealed that using the above molar ratio resulted in the formation of a 1D coordination polymer $\{[Co(pzdc)_2(H_2O)_2].H_2O\}_n$ ($2^{\emptyset}$) where adenine did not appear in the crystal structure. A search in the Cambridge Structural Database revealed that this coordination polymer (CP) has already been synthesized using two other alternatives to adenine; the first approach used 2-aminopyrazine, that extended the synthesis period to three months [23] and the second approach used NaOH [24]. Since adenine was not present in the crystal structure (neither 2-aminopyrazine in the previous research), a blank reaction, without the presence of adenine or any other bases, was carried out and interestingly the one-dimensional CP $2^{\emptyset}$ was obtained. The latter procedure is less expensive in comparison with the other two methods, therefore, CP $2^{\emptyset}$ could be considered as a candidate precursor for the fabrication of cobalt oxide nanoparticles.

The asymmetric unit of $2^{\emptyset}$ contains one Co(II) cation, one half of the $pzdc^{2-}$ ligand, one coordinated and one uncoordinated water molecule (Fig. 5s). The distorted octahedral environment around each Co(II) ion is occupied by two $pzdc^{2-}$ ligands and two water molecules in the axial positions. Each $pzdc^{2-}$ ligand bridges two

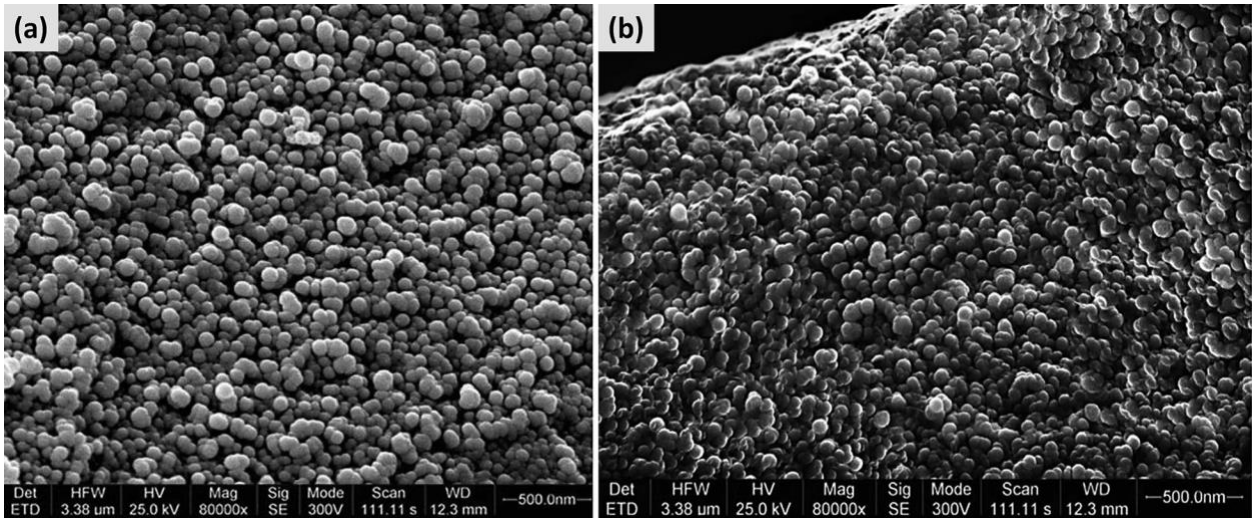


Fig. 1. SEM photographs of (a) compound 1 and (b) compound 2, prepared by sonochemical method.

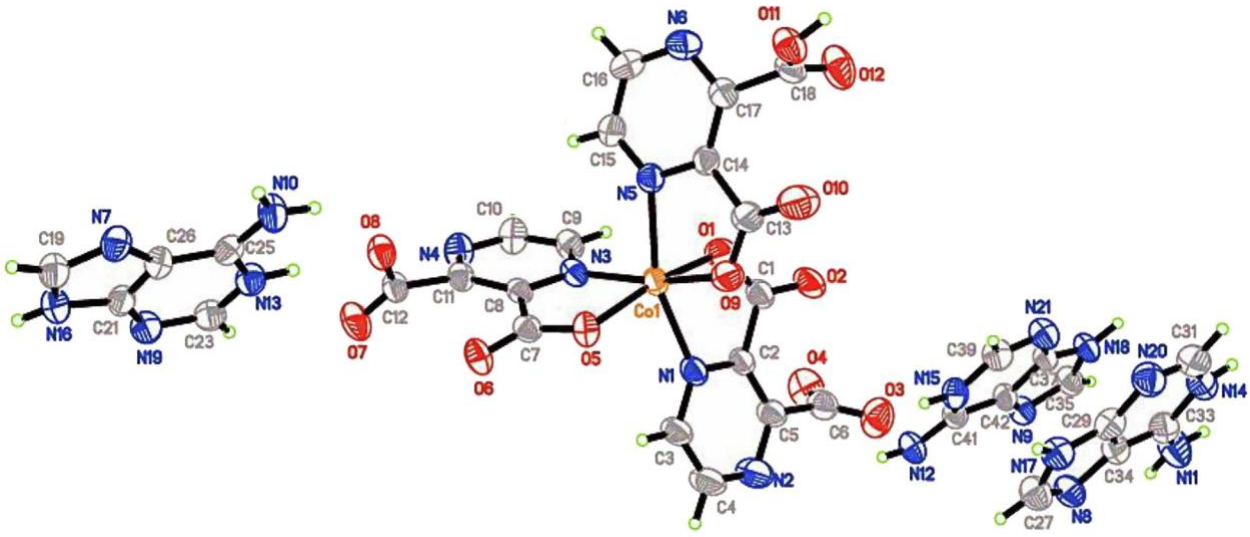


Fig. 2. The coordination environment of Co(II) cation in compound 1[◊]. (Due to clarity, water molecules were omitted).

cobalt ions and is coordinated to each one of them in a bidentate fashion through the nitrogen of the pyrazine ring and a carboxylate oxygen atom (Fig. 6s). The 1D polymeric chains are then connected to each other by uncoordinated water molecules through strong hydrogen bonds and build up a 3D architecture (Fig. 7s and Table 3s).

### 3.2. Characterization of 1 and 2

Fig. 3 illustrates the XRPD pattern of the typical sample of 1 prepared by the ultrasonic method in comparison with the simulated XRPD pattern from single crystal X-ray data of 1[◊]. XRPD pattern clearly confirms the presence of only one crystalline phase in the sample prepared using the ultrasonic method. Acceptable matches are observed for the patterns, indicating that the nanoscale aggregates of 1 has an identical structure to that of the single crystals of 1[◊].

Similarly, the XRPD pattern of the typical sample of 2 prepared by the ultrasonic method matches very well with the simulated XRPD pattern from single crystal X-ray data of 2[◊] (Fig. 4). This con- firms an identical structure for CP 2 obtained by the ultrasonic method to that of CP 2[◊] determined by single crystal diffraction.

In both 1 and 2, the IR spectra of the product produced by the sonochemical method and that of the single crystals produced by the reflux method matches well (Figs. 8s and 9s are for 1 and 2, respectively). As can be seen from Fig. 8s, the broad bands in the 2900–3500 $cm^{-1}$ region indicate the OAH stretching vibration of water molecules and carboxylic acid groups. Strong absorption bands in the 1753 and 1357 $cm^{-1}$ correspond to asymmetric and symmetric stretching carboxylate groups ($COO^{-}$). The difference between the asymmetric and symmetric stretches is $D\nu_1 = (\nu_{as} - \nu_{sym}) = 396\ cm^{-1}$ confirming that these groups are not coordinated to the metal ion [25]. Those carboxylate groups that are coordinated to the metal ion, have shifted slightly to the lower frequencies and

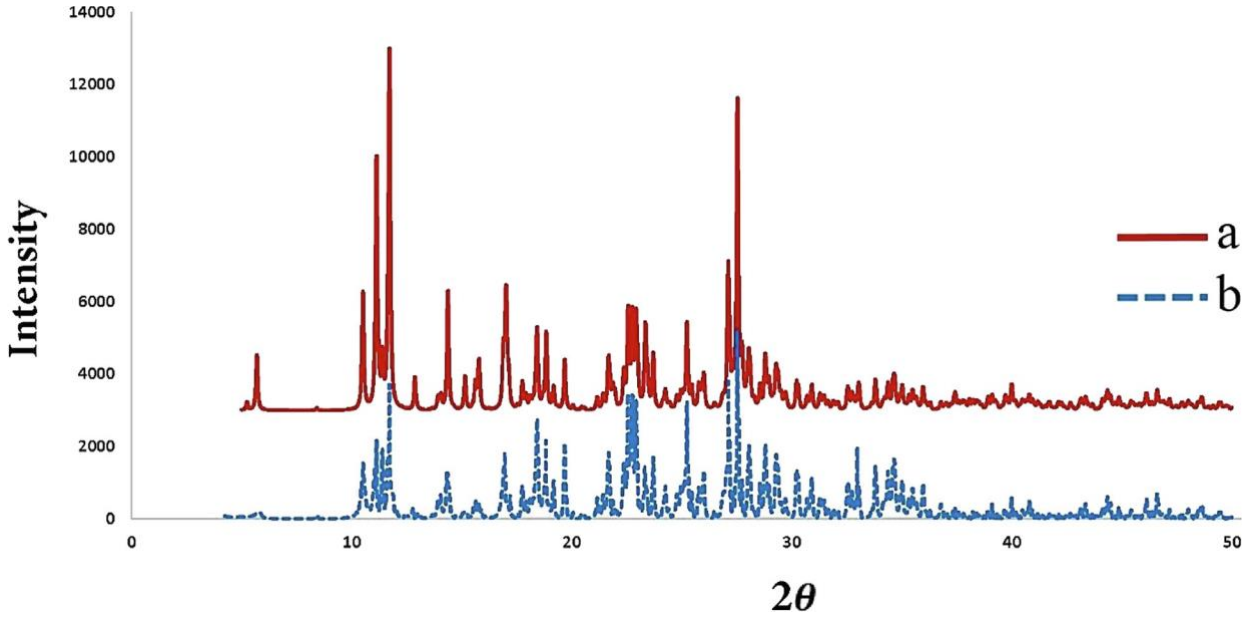


Fig. 3. XRD patterns of (a) simulated pattern based on single crystal X-ray data of compound 1[◊], (b) nanoscale aggregate of compound 1 prepared by sonochemical method.

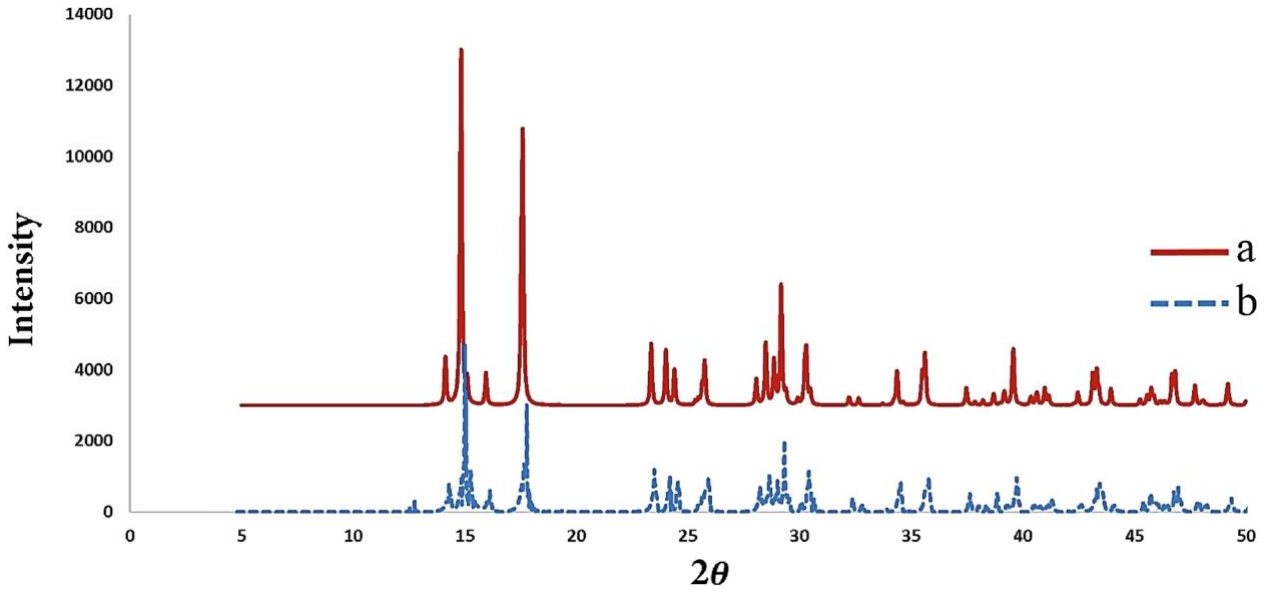


Fig. 4. XRD patterns of (a) simulated pattern based on single crystal X-ray data of compound 2', (b) nanoscale aggregate of compound 2 prepared by sonochemical method.

appear in 1612 and 1341 $cm^{-1}$. In this case the $\Delta\nu_2$ is 271 $cm^{-1}$, showing a decrease in comparison with $\Delta\nu_1$ and suggesting a monodentate binding of the carboxylate group to the cobalt(II) ion [26]. The peak in the 3375 $cm^{-1}$ confirms the presence of the amine group of the protonated adenine.

The spectra of compound 2 in Fig. 9s shows that the coordination of carboxylate groups to the Co(II) ions shifts the bands to lower frequencies of 1632 and 1377 $cm^{-1}$. A difference of $\Delta\nu_2$ = 255 $cm^{-1}$ indicates that the carboxylate groups are coordinated to the cobalt (II) center in a monodentate fashion.

### 3.3. Magnetic properties

In order to investigate the effect of particle size on the magnetic behavior of CP 2, its magnetic property was assessed and compared with the previously reported values for its single crystal counterpart (CP 2') [24]. DC magnetic susceptibility was measured for CP 2 in the temperature range of 2–300 K and in a constant tempera- ture of 2 K as a function of field.

The thermal dependence of $\chi T$ for CP 2 is shown in Fig. 5. The $\chi T$ value of 2.7 emu/K mol at 300 K for CP 2 is in agreement with the reported value for a Co(II) in a distorted octahedral coordination environment having strong spin–orbit coupling. There are several exchange pathways between coupled Co(II) ions *via* the pyrazine ring and *via* the carboxylato ligands. Also, the weak ferromagnetism observed at 495 Oe below 30 K might be caused by canting of the spins that are antiferromagnetically coupled. Since the Co(II) is *hexa*-coordinated in CP 2, it displays strong spin–orbit coupling and an effective spin of 1/2 at 2 K, with an effective g value of 4.33 (Fig. 6). When spin–orbit coupling is switched on, the ground state further has been split by zero-field and Kramers effects. Each Co(II) lies on the inversion center and the other cobalt ions in the chain are generated by a two-fold axis, thus the magnetic moments in the unit cell are not related by an inversion center, and therefore a build-up of spin due to spin canting is possible.

### 3.4. Metal oxide nanoparticles

Nanoparticles of $Co_3O_4$ have been prepared by thermal decomposition of CP 2 (prepared by the ultrasonic method) at different calcination temperatures of 400, 600, 800 and 850 °C. In Fig. 7, the XRPD patterns of the synthesized $Co_3O_4$ nanoparticles *via* the calcination process at different temperatures confirm the formation of $Co_3O_4$, as matches well with the standard pattern of $Co_3O_4$ (JCPDS card No. 98–001-0241). The reflection peaks in all cases are strong and sharp and confirm a single pure phase. The SEM images of the metal oxide obtained from the direct calcination of CP 2 at different calcination temperatures illustrated the formation of nanoscale $Co_3O_4$. Interestingly as shown in Fig. 8, the morphology of the $Co_3O_4$ products are quite temperature dependent *i.e.* calcination at 400 °C resulted in nano-belt morphology with a 50–90 nm size distribution (Fig. 8a) while $Co_3O_4$ nanoparticles prepared at 600 °C, appear as nano-rods with slight decrease in the size of particles from 30 to 80 nm (Fig. 8b). Fig. 8c shows selforganization of nano-rods into cauliflower-like morphology at 800 °C. With further increase in calcination temperature (850 °C), the cauliflower-like nanoparticles of $Co_3O_4$ disappears and a new ginger-like morphology with a 30–80 nm size distribution were formed (Fig. 8d).

## 4. Conclusions

Using an ultrasonic synthesis technique and by applying different molar ratios of PT to metal ions, two new nanoscale coordination compound $(adH)_3[Co(Hpzdc)(pzdc)_2].6H_2O$ (1) and $\{[Co(pzdc)_2(H_2O)_2].H_2O\}_n$ (2) have been synthesized and fully characterized. Compound 2 is a coordination polymer (CP) and is proved to be a suitable precursor for $Co_3O_4$ nanoparticles, to which it converts upon calcination at different temperatures ranging between 400 and 850 °C under atmospheric air. It is interesting that crystalline size and morphology of nanoscale $Co_3O_4$ are significantly influenced by calcination temperatures causing various nano-belt, nano-rod, cauliflower-like and ginger-like morphologies.

Moreover, a new synthesis procedure for CP 2 and its single crystal counterpart has been reported which makes it a relatively low-cost and readily available precursor for $Co_3O_4$ nanoparticles. Considering the structure of CP 2 as a 1D coordination polymer, the thermal dependency of magnetic susceptibility measurements indicates a strong spin–orbit contribution with the zero-field splitting effect of the high-spin Co(II) ions. It was also found that reduction of the particle size of CP 2 does not improve its magnetic properties.

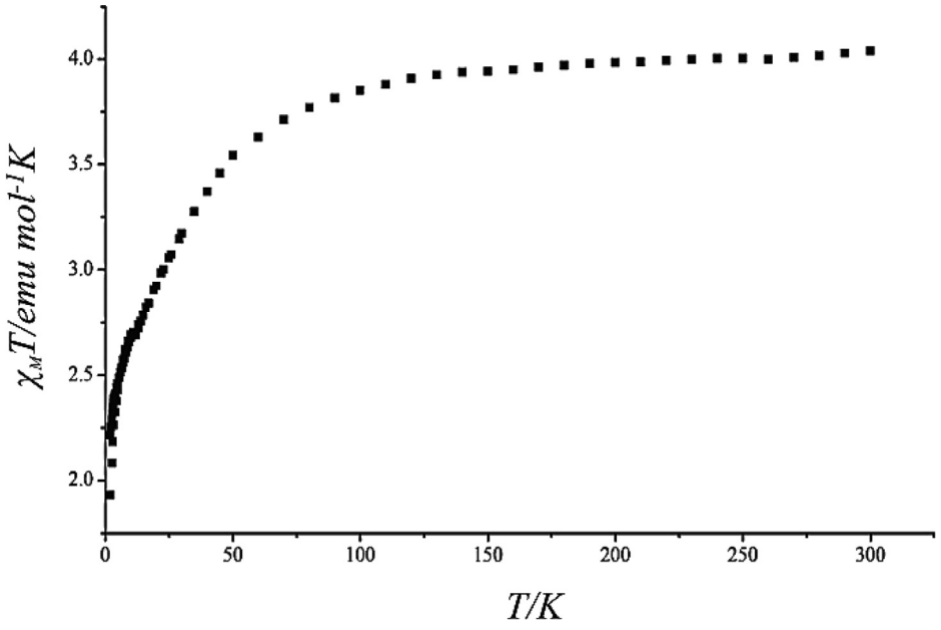


Fig. 5. $V_T$ vs. T plot for nanoscale aggregate of compound 2 at 495 Oe below 30 K and T between 2 and 300 K.

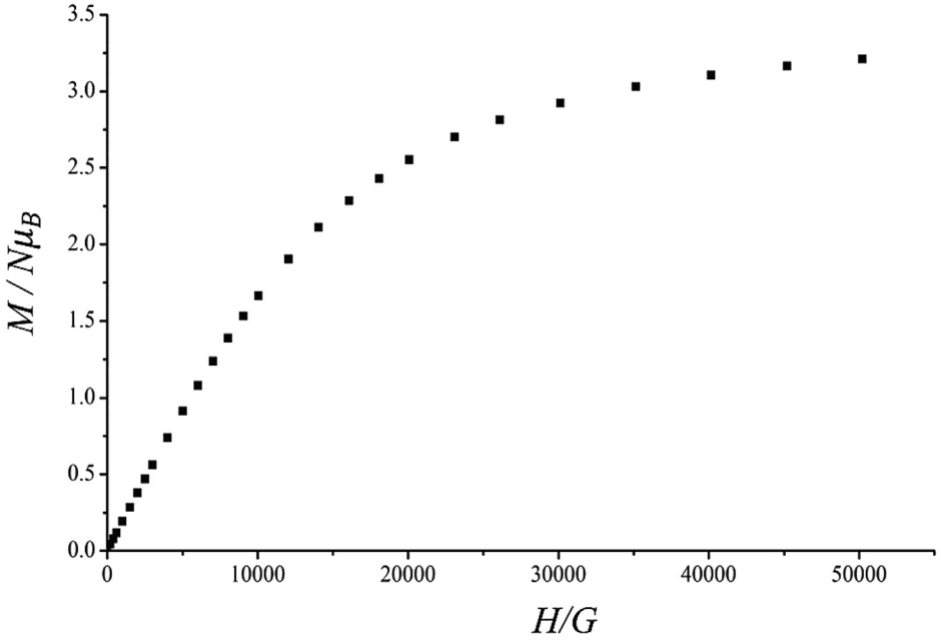


Fig. 6. Magnetization vs. field plot for nanoscale aggregate of compound 2 at 2 K.

## CRediT authorship contribution statement

Arash Farahmand Kateshali: Investigation, Writing - original draft. Janet Soleimannejad: Supervision, Conceptualization, Writing - review & editing. E. Carolina Sañudo: Formal analysis, Writing - review & editing.

## Declaration of Competing Interest

The authors declare that they have no known competing financial interests or personal relationships that could have appeared to influence the work reported in this paper.

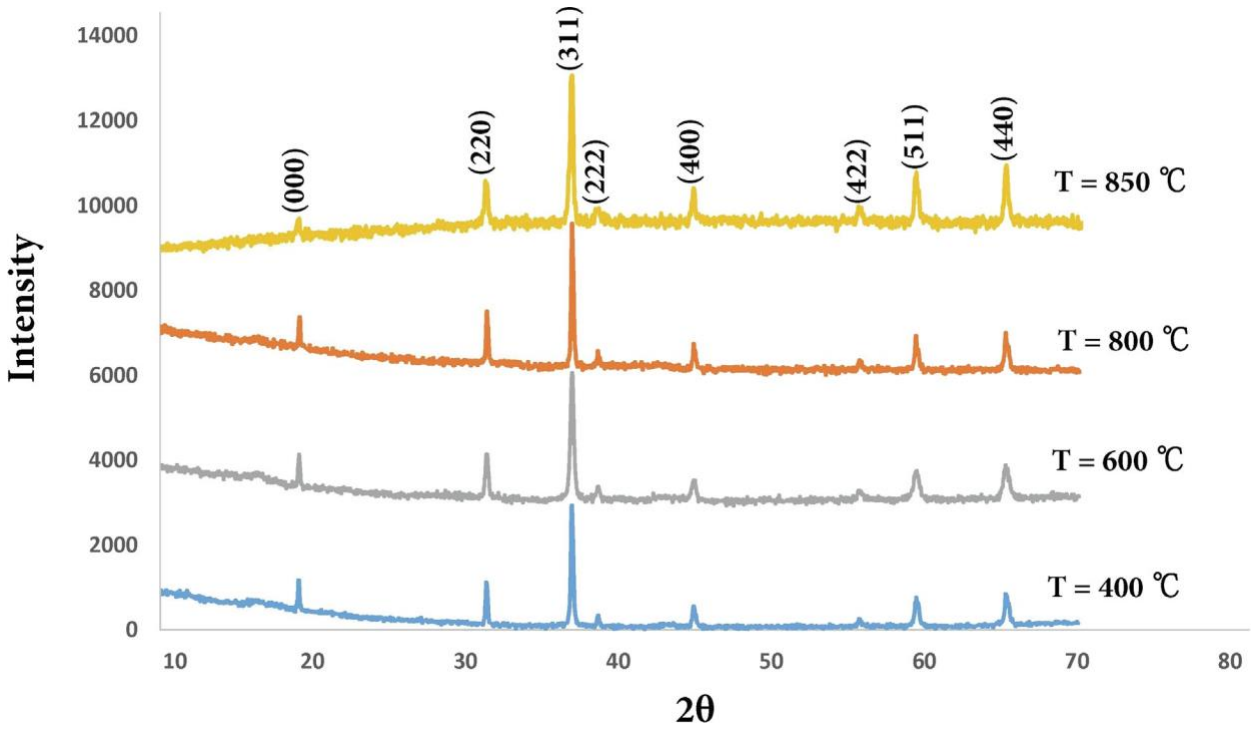


Fig. 7. XRD pattern of $Co_3O_4$ nanoparticles prepared from CP 2 at different calcination temperatures.

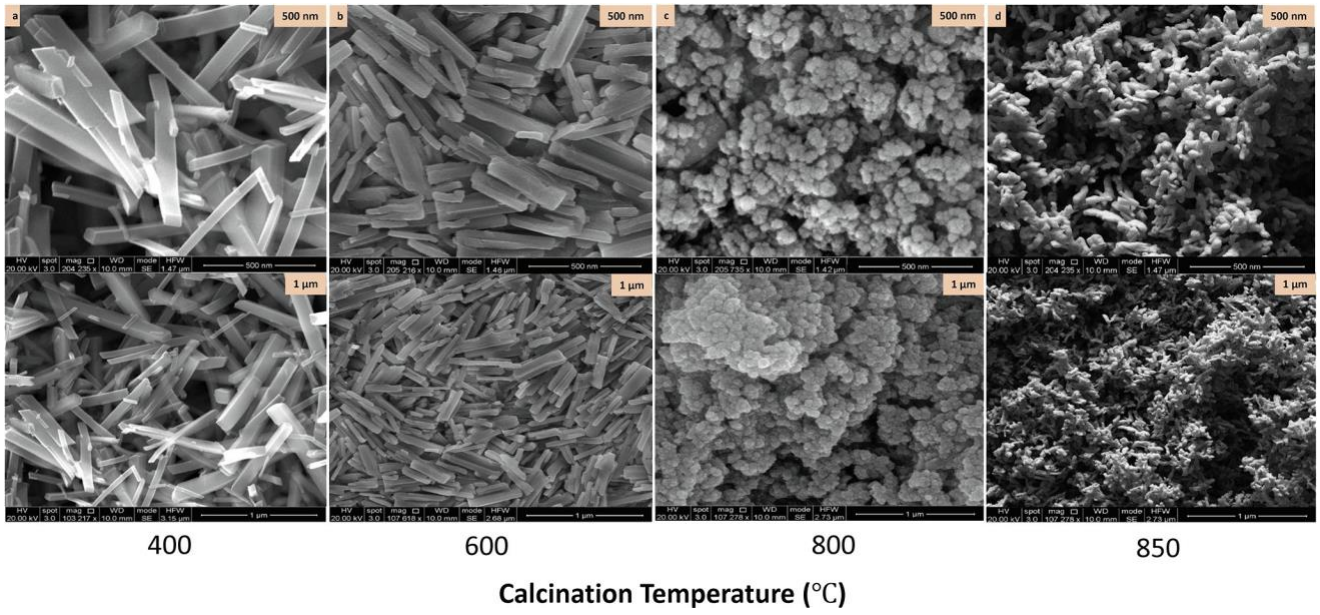


Fig. 8. SEM image of the $Co_3O_4$ nanoparticles prepared from CP 2 at different calcination temperatures (a) 400 °C, (b) 600 °C, (c) 800 °C, and (d) 850 °C.

## Acknowledgement

Funding for this research was provided by the University of Tehran.

## Appendix A. Supplementary data

Supplementary data to this article can be found online at https://doi.org/10.1016/j.poly.2020.114565.

## References

[1] N.V. Gorantla, V.G. Landge, P.G. Nagaraju, P. Priyadarshini CG, E. Balaraman, S. Chinnathambi, Molecular cobalt (II) complexes for TAU polymerization in Alzheimer's disease, ACS Omega, 4 (2019) 16702–16714.

[2] J. Gu, M. Wen, Y. Cai, Z. Shi, D.S. Nesterov, M.V. Kirillova, A.M. Kirillov, Cobalt (II) coordination polymers assembled from unexplored pyridine-carboxylic acids: structural diversity and catalytic oxidation of alcohols, Inorg. Chem. 58 (2019) 5875–5885.

[3] B. Gutiérrez-Tarriño, J.L. Olloqui-Sariego, J.J. Calvente, M. Palomino, G. MínguezEspallargas, J.L. Jordá, F. Rey, P. Oña-Burgos, Cobalt metal-organic framework

based on two dinuclear secondary building units for electrocatalytic oxygen evolution, ACS Appl. Mater. Interfaces 11 (2019) 46658–46665.
[4] R. Rajak, M. Saraf, S.M. Mobin, Mixed-ligand architected unique topological heterometallic sodium/cobalt-based metal-organic framework for high-performance supercapacitors, Inorg. Chem. 59 (2020) 1642–1652.
[5] Q.Q. Tu, L.L. Ren, Y.Y. Cui, A.L. Cheng, E.-Q. Gao, Assembly of four new cobalt coordination polymers modulated by N-coligands: sensitive and selective sensing of nitroaromatics, $Fe^{3+}$ and $Cr_2O_7^{2-}$ in water, CrystEngComm 22 (2020) 1789–1801.
[6] Q.Q. Xiao, G.Y. Dong, Y.H. Li, G.H. Cui, Cobalt (II)-based 3D coordination polymer with unusual 4,4,4-connected topology as a dual-responsive fluorescent chemosensor for acetylacetone and $Cr_2O_7^{2-}$, Inorg. Chem. 58 (2019) 15696–15699.
[7] F. Novio, J. Simmchen, N.V. Mera, L.A. Ferré, D.R. Molina, Coordination polymer nanoparticles in medicine, Coord. Chem. Rev. 257 (2013) 2839–2847.
[8] P. Horcajada, T. Chalati, C. Serre, B. Gillet, C. Sebrie, T. Baati, J.F. Eubank, D. Heurtaux, P. Clayette, C. Kreuz, J.S. Chang, Y.K. Hwang, V. Marsaud, P.N. Bories, L. Cynober, S. Gil, G. Férey, P. Couvreur, R. Gref, Porous metal–organic frame work nanoscale carriers as a potential platform for drug delivery and imaging, Nature Mat. 9 (2010) 172–178.
[9] K.S. Suslick, Mechanochemistry and sonochemistry: concluding remarks, Faraday Discuss. 170 (2014) 411–422.
[10] J.H. Bang, K.S. Suslick, Applications of ultrasound to the synthesis of nanostructured materials, Adv. Mater. 22 (2010) 1039–1059.
[11] F. Moghzi, J. Soleimannejad, Jan Janczak, Dual-emitting barium based metal-organic nanosheets as a potential sensor for temperature and anthrax biomarkers, Nanotechnology 31 (2020) 245706.
[12] F. Moghzi, J. Soleimannejad, Sonochemical synthesis of a new nano-sized barium coordination polymer and its application as a heterogeneous catalyst towards sono-synthesis of biodiesel, Ultrasonics Sonochem. 42 (2018) 193–200.
[13] S.D. Taherzade, J. Soleimannejad, A.A. Tarlani, Application of metal-organic framework nano-MIL-100(Fe) for sustainable release of doxycycline and tetracycline, Nanomaterials 7 (2017) 215–229.
[14] Y. Tang, A.C. Soares, M. Ferbinteanu, Y. Gao, G. Rothenberga, S. Tanase, Coordination polymers from alkaline-earth nodes and pyrazine carboxylate linkers, Dalton Trans. 47 (2018) 10071–10079.
[15] G. Beobide, O. Castillo, A. Luque, U.G. Couceiro, J.P.G. Teran, P. Roman, Supramolecular architectures and magnetic properties of coordination polymers based on pyrazine dicarboxylato ligands showing embedded water clusters, Inorg. Chem. 45 (2006) 5367–5382.
[16] S.R. Sushrutha, R. Hota, S. Natarajan, Adenine-based coordination polymers: synthesis, structure, and properties, Eur. J. Inorg. Chem. 18 (2016) 2962–2974.
[17] J.P.G. Teran, O. Castillo, A. Luque, U.G. Couceiro, G. Beobide, P. Roman, Molecular recognition of adeninium cations on anionic metal-oxalato frameworks: an experimental and theoretical analysis, Inorg. Chem. 46 (2007) 3593–3602.
[18] T. Kavitha, S. Haider, T. Kamal., M. Ul-Islam, Thermal decomposition of metal complex precursor as route to the synthesis of Co3O4 nanoparticles: antibacterial activity and mechanism, Alloy. Compd. 704 (2017) 296–302.
[19] H. Chen, M. Yang, S. Tao, G. Chen, Template-free synthesis of $Co_3O_4$ nanorings and their catalytic application, CrystEngComm. 20 (2018) 679–688.
[20] G.M. Sheldrick, SHELXS-97, SHELXL-97. Program Package for Crystal Structure Solution and Refinement, University of Göttingen, Göttingen, Germany, 1997.
[21] G.M. Sheldrick, A short history of SHELX, Acta Cryst. A. 64 (2008) 112.
[22] SHELXTL 5.1, Bruker Analytical X-Ray Instruments, Inc., 1998.
[23] M. Mirzaei, H.E. Hosseini, A. Bauzá, S. Zarghami, P. Ballester, J.T. Maguee, A. Frontera, On the importance of non covalent interactions in the structure of coordination Cu(II) and Co(II) complexes of pyrazine- and pyridine-dicarboxylic acid derivatives: experimental and theoretical views, CrystEngComm. 16 (2014) 6149–6158.
[24] L. Mao, S.J. Rettig, R.C. Thompson, J. Trot, S. Xia, 2,3-Pyrazinedicarboxylates of cobalt(II), nickel(II), and copper(II); magnetic properties and crystal structures, Can. J. Chem. 74 (1996) 433–444.
[25] O.Z. Yesilel, A. Mutlu, O. Büyükgüngör, A new coordination mode of 2,3-pyrazinedicarboxylic acid and its first monodentate complexes, Polyhedron. 27 (2008) 2471–2477.
[26] K. Nakamoto, Infrared and Raman Spectra of Inorganic and Coordination Compounds, 5th ed., Wiley Interscience, New York, 1997, pp. 59–62.